31st Annual International Conference of the IEEE EMBS
Minneapolis, Minnesota, USA, September 2-6, 2009

Real-time implementation of biofidelic SA1 model for tactile feedback

A. F. Russell, R. S. Armiger, R. J. Vogelstein, S. J. Bensmaia and R. Etienne-Cummings

Abstract—**In order for the functionality of an upper-limb prosthesis to approach that of a real limb it must be able to, accurately and intuitively, convey sensory feedback to the limb user. This paper presents results of the real-time implementation of a 'biofidelic' model that describes mechanotransduction in Slowly Adapting Type 1 (SA1) afferent fibers. The model accurately predicts the timing of action potentials for arbitrary force or displacement stimuli and its output can be used as stimulation times for peripheral nerve stimulation by a neuroprosthetic device. The model performance was verified by comparing the predicted action potential (or spike) outputs against measured spike outputs for different vibratory stimuli. Furthermore experiments were conducted to show that, like real SA1 fibers, the model's spike rate varies according to input pressure and that a periodic 'tapping' stimulus evokes periodic spike outputs.**

I. Introduction

According to the National Limb Loss Information Centre there are 1.9 million amputees living in the United States of America with an estimated 12 500 new upper limb amputations occurring every year [1]. Consequently, there exists a large need for an upper limb prosthesis which can match the performance of a real limb. Large advances have been made in the field of decoding neural signals to predict arm and finger movements [2-5], but the success in providing intuitive sensory feedback to the limb user has been limited.

In the intact limb, the glabrous skin of the fingertips is largely responsible for conveying tactile feedback during normal hand movements. The skin is innervated by three types of afferent nerve fibers: slowly adapting type 1 (SA1), rapidly adapting (RA) and Pacinian (PC) fibers. Each of these fibers conveys different information about the deformation of the skin to the brain. SA1 fibers respond to low frequency vibrations (taps) and pressure, and convey form and texture information. RA fibers convey information necessary for grip control and respond to intermediate frequencies and to motion across the skin. PC fibers respond to high frequency vibrations and convey information about distal events such as when sensing through a tool [6]. For a review of these fibers see [7].

To provide intuitive sensory feedback to a prosthetic limb user, stimulation of the sensors should activate the above fibers in the manner in which a stimulus to the intact hand would. However, most prosthetic technologies do not allow for this. Instead sensory feedback, if present at all, is provided through the use of tactors. In this feedback modality, tactile sensations are encoded and then applied to the user's skin through mechanical stimulation, in a region that has normal or near normal sensory capacity. In targeted sensory reinnervation, where nerves that normally innervate the hand are remapped to the skin of the residual limb, tactor-based feedback has the potential to elicit sensations projected to the phantom of the hand [8]. However, in most cases tactor-based feedback is unnatural and the user has to learn to associate the applied stimulus with the missing limb [9]. Furthermore, the mechanoreceptor density of the reinnervated skin is lower than that of the fingers so the resolution of the feedback is lower when applied to the former than if it emanated from the latter.

An alternative method is to stimulate the peripheral nervous system directly. Vallbo *et al.* [10], and Ochoa and Torebjork [11] have shown that stimulation of individual afferent fibers evokes a percept that is referred to the location of the afferent's receptive field and corresponds to the type of afferent stimulated. For example activating SA1 afferents with a continuous stimulus results in the sensation of sustained skin pressure. Peripheral nerve stimulation thus elicits more natural sensations than do other methods [12]. Three major difficulties, however, hamper this approach. The first is the ability to isolate individual afferent fibers for stimulation, the second is the ability to evoke a single action potential in the afferent fiber and the last is deciding on the temporal pattern of activation to apply to the nerve fiber given a stimulus. Advances in microelectrode arrays such as the Utah slant array [13]have helped address the first two issues. The third issue can be addressed by assuming that producing the same action potential sequence in the fiber that would be produced in the intact limb by the stimulus will elicit natural percepts of the stimulus. We have developed a model of the SA1 system that can accurately predict spike times for an arbitrary input stimulus [14].

This work was sponsored by the Johns Hopkins University Applied Physics Laboratory under the DARPA Revolutionizing Prosthetics program; contract N66001-06-C-8005.

A. F. Russell (Corresponding author: alexrussell@jhu.edu), R. J. Vogelstein and R. Etienne-Cummings are with the Department of Electrical and Computer Engineering at Johns Hopkins University, Baltimore, MD, USA, 21218.
S. J. Bensmaia is with the Krieger Mind/Brain Institute at the Johns Hopkins University, Baltimore, MD, USA, 21218.
R. S. Armiger and R. J. Vogelstein are with the Johns Hopkins Applied Physics Laboratory, Laurel, MD, USA, 20723.

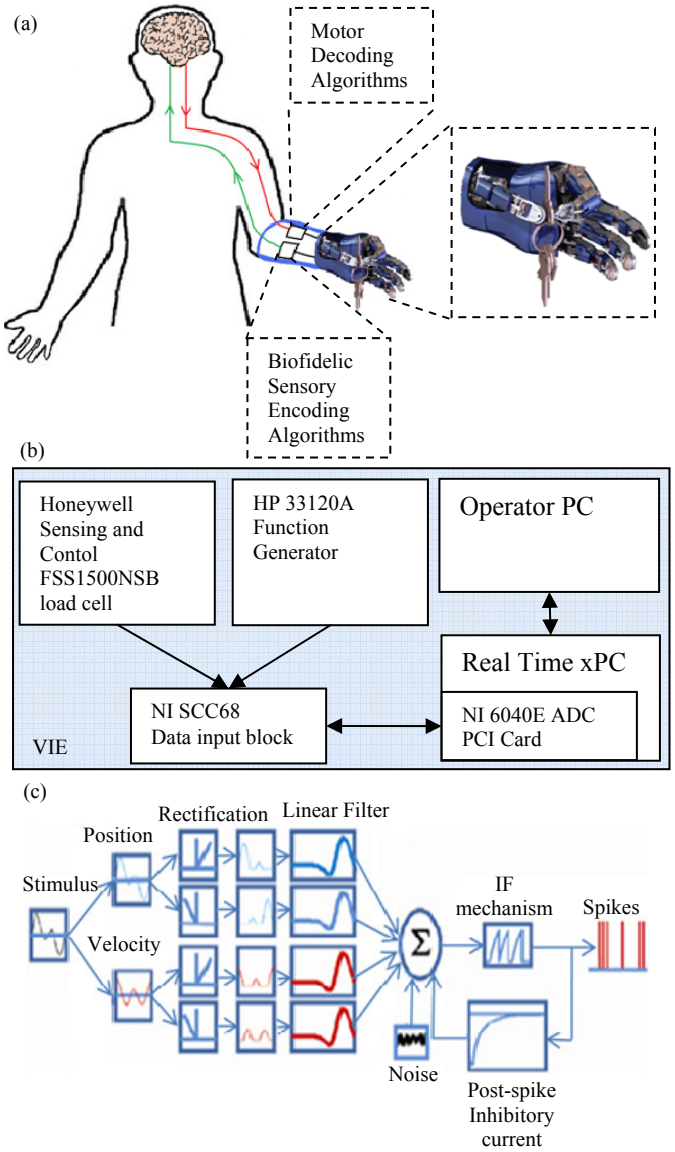

Figure 1: (a) Information flow through the prosthetic system. Motor decoding algorithms will use efferent nerve (red) signals to predict the desired movement of the limb. Sensory feedback will be encoded using biofidelic algorithms and transmitted to the brain through afferent nerve (green) stimulation (Image courtesy of JHU-APL). This feedback is envisioned to be implemented as follows: arrays of electrodes will be implanted into the residual ulnar and median nerves of the amputated arm. Next, fibers stimulated by the electrodes will be classified by type and projected field. Finally, the temporal pattern of stimulation for SA1 afferents will be generated through the use of the real-time model described in this paper. (b) Block diagram of the experimental setup using the VIE system (c) Leaky and Noisy Integrate and Fire Neuron model. The model accepts a displacement stimulus. This stimulus along with its first derivative are split into their positive and negative components and filtered. The summation of the filtered components then forms the input to the IF neuron.

These spike times can then be used as the stimulation pattern for sensory feedback.

The remainder of this paper describes the real-time implementation of this model in a Virtual Integration Environment (VIE) [15] and the coupling of this model with external sensors.

II. Methods

A. The Virtual Integration Environment

The Virtual Integration Environment (VIE) was developed by the Johns Hopkins University Applied Physics Laboratory (Laurel, MD, USA) for the prototyping of algorithms for the control of a 22 degree of freedom prosthetic arm [15]. The VIE is implemented using the Simulink toolbox for MATLAB 2008b (Mathworks Inc, Natick, MA, USA). The control algorithms for the arm are developed in Simulink and then compiled to run on a real-time PC (xPC). The xPC controls the virtual limb and can interact with external sensors through a NI 6040E ADC PCI card. The limb model incorporates limb dynamics and kinematics which were designed to mimic the mechanical and physical properties of the limbs being developed for the DARPA Revolutionizing Prosthetics 2009 project. The limb consists of a comprehensive model of the human arm developed using MusculoSkeletal Modeling Software (MSMS) [16, 17]. The VIE physics engine allows for basic interactions between the arm and objects. These interactions could be extended to provide a virtual haptic environment. The virtual arm and environment could then be used to perform closed loop motor-decoding/sensory-encoding experiments. For a more detailed description of the VIE see [15]. For the experiments described here, the xPC was configured to run with a step size of 1ms.

B. The model

Only a brief description of the model will be given as it has previously been discussed in [14]. The model consists of a rectification and filter stage followed by a noisy, leaky Integrate and Fire (IF) neuron. The model is driven by position and its first derivative, velocity, which have been found to be sufficient to predict responses. Because the IF neuron allows only for linear transforms of its inputs, the position and velocity inputs are separated into their positive and negative components, allowing for separate linear transforms on each component. Each of these four components is then filtered and the outputs of the filters are summed to form the input current for the IF neuron. Gaussian noise is also injected into the neuron at this stage. When the membrane potential V reaches a threshold ($V_{thresh} = 1$) then an action potential is produced ($Spike = 1$)and the membrane voltage is reset ($V = V_{reset} = 0$). The differential equations governing the dynamics of the IF neuron were written as difference equations to ease the computational load on the xPC. The dynamics are as follows:

$$
\begin{aligned}
&if\ V[z^{-1}] > V_{thresh}\ then \\
&\qquad V[z] = (V[z^{-1}] - V_{leak})D_1 + V_{leak} + I_{net}D_2 + \sigma N \\
&\qquad spike = 1 \\
&else \\
&\qquad V[z] = V_{leak}(1 - D_1) + V_{reset}D_1 + I_{net}D_2 + \sigma N \\
&\qquad spike = 0 \\
&end
\end{aligned}
$$

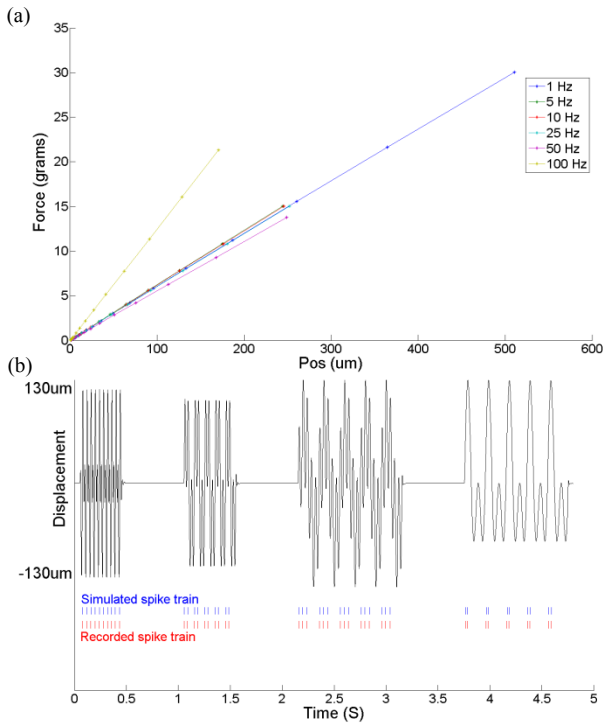

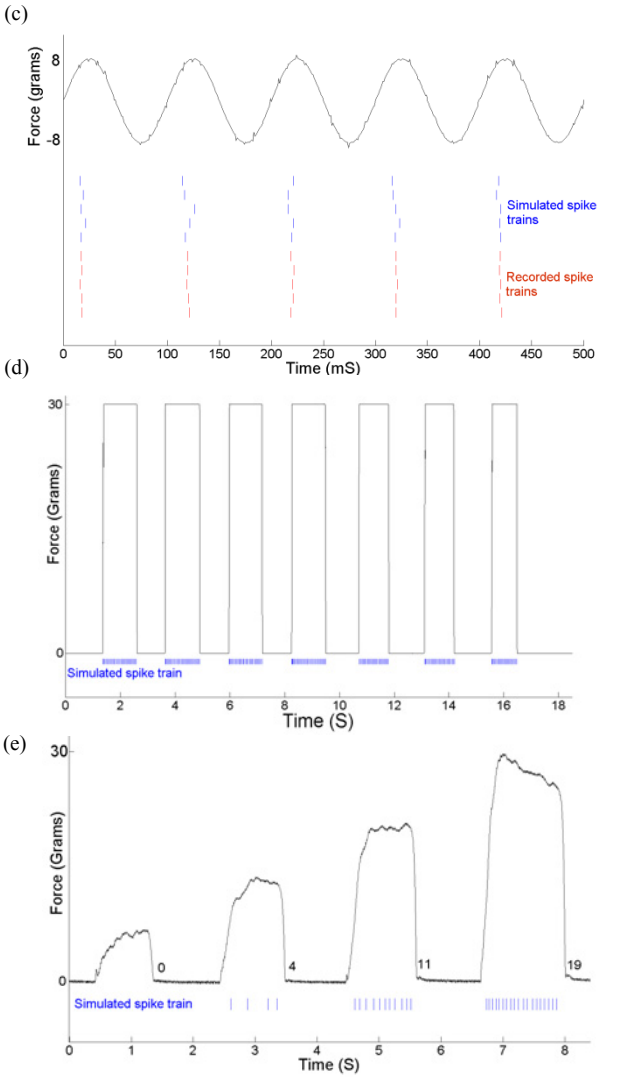

Figure 2: (a) Force required to produce a given indentation into the finger pad of a monkey at varying frequencies. (b) Predicted (blue) and measured (red) spike trains evoked by 4 vibratory stimuli (black trace) (c) Predicted response (blue) and measured response (red) to a 10Hz sinusoid with a zero-to-peak force of 8grams (which corresponds to a zero-to-peak displacement of 130μm). Each row of the measured or predicted responses corresponds to the responses evoked by successive applications of the same stimulus (to the skin or the model). (d) Model responses when the load cell is tapped repeatedly (e) Predicted response to varying pressures applied to the load cell. The black trace is the load cell output. The number of spikes generated by each pressure stimulus is indicated next to the corresponding force deflection. The model response (spike rate) increases with force as is expected given the nature and function of SA1 afferent fibers

In figures (b) – (e) the predicted spike trains have been shifted back by the buffering time (60ms) to align the predicted data with the measured data and the stimuli.

$where\ D_1 = e^{-\frac{1}{\tau}}\ and\ D_2 = \tau\left(1 - e^{-\frac{1}{\tau}}\right)$
$and\ I_{net} = I_{in} + I_{ps}$

V_{leak} is the leak potential of the neuron, N is the Gaussian noise, σ is the standard deviation of the noise, D_1 is the decay of the membrane voltage and D_2 is the decay of the contribution of I_{net} to the membrane voltage, τ is the membrane time constant in ms. I_{ps} is a post spike inhibitory current accumulated over all past spikes and I_{in} is the input current from the filtering stage, given by:

$$I_{in}(z) = \sum_{i=0}^{1}(H_i^+(z) * y_i^+(z) + H_i^-(z) * y_i^-(z))$$

Where $y_i^+(z)$ and $y_i^-(z)$ are the positive and negative components of the i^{th} derivative of position and $H_i^+(z)$ and $H_i^-(z)$ are the corresponding linear filters. Each filter has 60 coefficients and so a buffer of 60ms was added to the front of the model to ensure correct filtering during real-time operation. The parameters for the above model were found using an approach developed by Paninski and Pillow [18, 19]involving density propagation techniques.

C. *Force-Displacement Conversion*

Because the sensors on a prosthetic arm are more likely to sense force than displacement an additional block was added to the Simulink model to transform a sinusoidal input force into the corresponding displacement. The conversion factor was calculated by measuring the force required to cause different indentation amplitudes to a Rhesus Macaque's distal finger pad at frequencies of 1, 5, 10, 25, 50 and 100Hz (see Figure 2a). The slope (m) of each of the force-amplitude curves can then be used to find the displacement amplitude of the skin as follows:

$$Displacement = m \times force$$

D. *Testing the model*

Four input types were used to test the model. The first involved applying vibratory stimuli to the model and comparing the model results to recorded spike trains (from an anesthetized Rhesus macaque) evoked using the same stimuli (The afferent fiber from which the recordings were made innervated the glabrous skin of the hand. For a full description of the experimental procedure see [20]).The

second stimulus was a force input consisting of a 10Hz sinusoid with amplitude of 8 grams applied to the model through the ADC. This input was generated using an HP 33120A Function Generator. The force conversion outlined above was used to transform the force into displacement and the results of the model were compared to the recorded spike trains as in the previous experiment. The third and fourth inputs used the load cell to characterize the simulated response to taps and to various levels of pressure.

III. Results and Discussion

Figure 2(a) shows preliminary results from the force-displacement conversion experiment. It can be seen that at each frequency the force-displacement relationship is linear allowing a very simple transfer function to be used. Furthermore the slope is approximately independent of frequency for frequencies between 1 and 50Hz but increases abruptly at 100Hz. We are currently investigating the relationship between force and displacement more systematically and across a wider range of stimulus conditions. Figure 2(b) shows the responses of an SA1 afferent to 4 vibratory stimuli along with the responses predicted by the model. Model predictions match the measured responses almost perfectly, thereby bolstering the assertion that the model outputs are in fact 'biofidelic' (The average discrepancy between the model and the recorded spike trains is 0.2ms. For details see [14]). Figure 2(c) shows the predicted and measured responses to a simple sinusoid. The responses are closely matched showing that the model still has excellent performance when an external force input is applied. As mentioned above a more complete analysis of the relationship between force and displacement needs to be conducted before more complex force inputs can be tested.

Whilst there are no corresponding neurophysiological data to which to compare the results shown in Figures 2(d) - (e), these data show that the simulated SA1 afferent exhibits two critical properties observed *in vivo* of afferents of its type. Figure 2(d) shows that the simulated afferent responds to periodic taps applied to the load cell by firing periodic bursts of action potentials, as do SA1 afferents when their receptive fields are stimulated in this fashion. Figure 2(e) shows that the magnitude of the response of the simulated afferents (i.e. the number of spikes) to pressure stimuli applied to the load cell depends on the magnitude of the applied pressure. The simulated afferent thus conveys information about pressure in the same way as an SA1 afferent innervating the glabrous skin would.

IV. Conclusions

In the present study we develop a real-time algorithm for encoding sensory feedback which can be used for peripheral nerve stimulation in neural prostheses. Because this model was developed within the VIE, the algorithm can be readily compiled to an embedded device for use once sensor and nerve stimulation technologies have sufficiently evolved. Analogous models are currently being developed to simulate the responses of the other types of mechanoreceptive and thermoreceptive afferents innervating the skin.

V. References

[1] National Limb Loss Information Centre, "Amputation statistics by cause: limb loss in the United States," 2008, http://www.amputee-oalition.org/fact_sheets/amp_stats_cause.pdf.

[2] L. R. Hochberg, M. D. Serruya, G. M. Friehs, J. A. Mukand, M. Saleh, A. H. Caplan, A. Branner, D. Chen, R. D. Penn, and J. P. Donoghue, "Neuronal ensemble control of prosthetic devices by a human with tetraplegia," *Nature,* vol. 442, pp. 164-171, 2006.

[3] M. Velliste, S. Perel, M. C. Spalding, A. S. Whitford, and A. B. Schwartz, "Cortical control of a prosthetic arm for self-feeding," *Nature,* vol. 453, pp. 1098-1101, 2008.

[4] V. Aggarwal, S. Acharya, F. Tenore, H. Shin, R. Etienne-Cummings, M. Schieber, and N. Thakor, "Asynchronous decoding of dextrous finger movements using M1 neurons," *IEEE TNSRE,* vol. 6, pp. 3-14, 2008.

[5] B. M. Yu, C. Kemere, G. Santhanam, A. Afshar, S. I. Ryu, T. H. Meng, M. Sahani, and K. V. Shenoy, "Mixture of Trajectory Models for Neural Decoding of Goal-Directed Movements," *J Neurophysiol,* vol. 97, pp. 3763-3780, May 1, 2007 2007.

[6] G. Westling and R. Johansson, "Responses in glabrous skin mechanoreceptors during precision grip in humans," *Exp. Brain Res.,* vol. 66, pp. 128-140, 1987.

[7] K. Johnson , T. Yoshioka, and F. Vega-Bermudez, "Tactile Functions of Mechanoreceptive Afferents Innervating the Hand," *J of Clinical Neurophysiology,* vol. 17, pp. 539-558, 2000.

[8] T. Kuiken, L. Miller, R. Lipschutz, B. Lock, K. Stubblefield, P. Marasco, P. Zhau, and G. Dumanian, "Targeted reinnervation for enhanced prosthetic arm function in a woman with a proximal amputation: a case study," *Lancet,* vol. 369, pp. 371-380, 2007.

[9] R. Riso, A. Ignagni, and M. Keith, "Cognitive Feedback Use with FES Upper Extremity Neuroprostheses," *IEEE Transactions on Biomedical Engineering,* vol. 38, pp. 29-38, 1991.

[10] A. B. Vallbo, K. A. Olsson, K. G. Westberg, and F. J. Clark, "Microstimulation of single tactile afferents from the human hand: Sensory attributes related to unit type and properties of receptive fields," *Brain,* vol. 107, pp. 727-749, September 1 1984.

[11] J. Ochoa and E. Torebjork, "Sensations evoked by intraneural microstimulation of single mechanoreceptor units innervating the human hand," *Journal Physiology,* vol. 342, pp. 633-654, 1983.

[12] R. Riso, "Strategies for providing upper extremity amputees with tactile and hand position feedback- moving closer to the bionic arm," *Technology and Healthcare,* vol. 7, pp. 401-409, 1999.

[13] A. Branner, R. B. Stein, and R. A. Normann, "Selective Stimulation of Cat Sciatic Nerve Using an Array of Varying-Length Microelectrodes," *J Neurophysiol,* vol. 85, pp. 1585-1594, April 1, 2001 2001.

[14] S. Bensmaia, S. Kim, S, and A. Sripati, "Conveying tactile feedback using a model of mechanotransduction," *IEEE BIOCAS*, 2008.

[15] W. Bishop, R. Armiger, J. Burck, M. Bridges, J. Vogelstein, J. Beaty, and S. Harshbarger, "A Real-Time Virtual Integration Environment for the Design and Development of Neural Prosthetic Systems," *IEEE EMBS 2008*.

[16] R. Davoodi and G. Loeb, "A Software Tool for Faster Development of Complex Models of Musculoskeletal Systems and Sensorimotor Controllers in Simulink," *J Applied Biomechanics,* vol. 18, 2002.

[17] R. Davoodi, C. Urata, E. Todorov, and G. Loeb, "Development of *clinician*-friendly software for musculoskeletal modeling and control," *IEEE EMBS*, 2004, pp. 4622-4625.

[18] L. Paninski, J. Pillow, W, and E. Simoncelli, P, "Maximum likelihood estimation of a stochastic integreat-and-fire neural encoding model," *Neural Comp.,* vol. 16, pp. 2533-2561, 2004.

[19] J. Pillow, W, "Likelihood-based approaches to modeling the neural code," *Bayesian Brain: Probabilistic Appraches to Neural Coding*, K. Doya, S. Ishii, A. Pouget, and R. Rao, P, Eds. Boston MIT press, 2007, pp. 53-70.

[20] M. Muniak, A, S. Ray, S. Hsiao, S, J. Dammann, F, and S. Bensmaia, J, "The neural coding of Stimulus intensity: linking the population response of mechanoreceptive afferents with psychophysical behaviour," *J Neurosci,* vol. 27, pp. 11687-11699, 2007R. J. Vidmar. (1992, August).